A Sequential Bayesian Approach for Remaining Useful Life Prediction of Dependent Competing Failure Processes

Mengfei Fan, Zhiguo Zeng, Enrico Zio, Rui Kang, Ying Chen

A Sequential Bayesian Approach for Remaining Useful Life Prediction of Dependent Competing Failure Processes

Mengfei Fan, Zhiguo Zeng, Enrico Zio, *Senior Member, IEEE*, Rui Kang, and Ying Chen

***Abstract*—A sequential Bayesian approach is presented for remaining useful life (RUL) prediction of dependent competing failure processes (DCFP). The DCFP considered comprises of soft failure processes due to degradation and hard failure processes due to random shocks, where dependency arises due to the abrupt changes to the degradation processes brought by the random shocks. In practice, random shock processes are often unobservable, which makes it difficult to accurately estimate the shock intensities and predict the RUL. In the proposed method, the problem is solved recursively in a two-stage framework: in the first stage, parameters related to the degradation processes are updated using particle filtering, based on the degradation data observed through condition monitoring; in the second stage, the intensities of the random shock processes are updated using the Metropolis–Hastings algorithm, considering the dependency between the degradation and shock processes, and the fact that no hard failure has occurred. The updated parameters are, then, used to predict the RUL of the system. Two numerical examples are considered for demonstration purposes and a real dataset from milling machines is used for application purposes. Results show that the proposed method can be used to accurately predict the RUL in DCFP conditions.**

***Index Terms*—Degradation, dependent competing failure processes, Markov chain Monte Carlo, particle filtering, prognostics, random shocks, remaining useful life.**

Nomenclature

Acronyms and Abbreviations

AER	Average error rate.
CDF	Cumulative density function.
DCFP	Dependent competing failure processes.
HPP	Homogeneous Poisson process.
MCMC	Markov chain Monte Carlo.
MH	Metropolis-Hastings.
PF	Particle filtering.
PDF	Probability density function.
RUL	Remaining useful life.
TTF	Time-to-failure.
TTSF	Time-to-soft-failure.
TTHF	Time-to-hard-failure.

Notation

x	Natural degradation level.
z	Cumulative degradation level.
y	Observed degradation level.
η	Degradation rate (unknown constant with time-dependent noise).
S	Shock damage (unknown constant with time-dependent noise).
λ	Shock intensity (unknown constant).
W	Shock load (random variable).
D	Load threshold of fatal shocks (constant).
ω	Process noise (random variable).
ν	Observation noise (random variable).
τ	Testing period.
M	Number of particles in the PF algorithm.
N_S	Number of MCMC samples.
N_M	Number of measurement points.

Manuscript received November 22, 2017; revised May 15, 2018 and August 21, 2018; accepted October 3, 2018. This work was supported in part by the National Natural Science Foundation of China under Grant 61573043, Grant 71671009, and Grant 71601010, and in part by the China Scholarship Council (201606020082). Associate Editor: Y. Deng. *(Corresponding author: Zhiguo Zeng.)*

M. Fan, R. Kang, and Y. Chen are with the School of Reliability and Systems Engineering, Beihang University, Beijing 100083, China (e-mail: fanmengfei@buaa.edu.cn; kangrui@buaa.edu.cn; cheny@buaa.edu.cn).

Z. Zeng is with the Chair on System Science and the Energy Challenge, Fondation Electricite de France, Laboratoire Genie Industriel, CentraleSupelec, Universite Paris-Saclay, Gif-sur-Yvette 4103, France (e-mail: zhiguo.zeng@centralesupelec.fr).

E. Zio is with the Chair on System Science and the Energy Challenge, Fondation Electricite de France, Laboratoire Genie Industrie, CentraleSupelec, Universite Paris-Saclay, Gif-sur-Yvette 4103, France, and also with the Energy Department, Politecnico di Milano, Milano 20133, Italy (e-mail: enrico.zio@ecp.fr).

Color versions of one or more of the figures in this paper are available online at http://ieeexplore.ieee.org.

Digital Object Identifier 10.1109/TR.2018.2874459

I. Introduction

SYSTEMS are often subject to multiple dependent competing failure processes (DCFP) [1]. In DCFP, a failure can be either a soft failure, caused by gradual degradation processes, or a hard failure, caused by catastrophic events [2], [3]. A key feature of DCFP is that dependencies often exist among failure processes. For instance, wear of metal components might increase the likelihood of fracture, since structural strengths are reduced by wear. When DCFPs exist, conventional reliability assessment methods would produce over-optimistic results, as they are based on assumptions of independence. For this reason, modeling of DCFP has lately received attention in system reliability analysis [4].

In literature, various models have been proposed for DCFP. Peng *et al.* [4] developed a reliability model for DCFP where

a shock brings a sudden increase to the degradation process. Wang and Pham [5] considered a similar system and developed a multiobjective optimization method to determine the optimal imperfect preventive maintenance policy for such a system. Wang *et al.* [6] considered another type of dependency where a shock changes the failure rate. Jiang *et al.* [7] investigated reliability and maintenance modeling for DCFP, where the threshold of hard failures is shifted by random shocks. Rafiee *et al.* [8] developed a DCFP model in which the degradation rates are shifted by different shock patterns. In [9], three possible effects of nonfatal shocks, *i.e.*, inducing degradation increments, accelerating degradation rates, and reducing hard failure thresholds, were considered in a comprehensive DCFP model. Lin *et al.* developed a multistate physics model [10] for DCFP considering both extreme shocks, which lead to the hard failure, and cumulative shocks, which affect degradation rates. Song *et al.* [11] classified shocks into different sets and developed a reliability model for multicomponent systems influenced by distinct shock sets. Jiang *et al.* [12] categorized shocks into safety, damage and fatal shock zones based on their magnitudes, and considered different effects of zone shocks on the degradation process. In [13]–[15], models were developed for DCFPs where the probability of hard failures is increased as the degradation process progresses. Huynh *et al.* [16], [17] investigated maintenance strategies for DCFP where the intensity of the random shock process is a piecewise function of the degradation magnitude. This type of dependency was also considered by Caballe *et al.* [18] in their research on condition-based maintenance planning for DCFP. Fan *et al.* [19] presented a reliability model for sliding spools where the dependency between the intensity of the random shock process and the degradation level is characterized by a linear function. The same authors also developed a stochastic hybrid systems-based modeling framework [20] for multiple types of dependencies and efficient reliability evaluation. Zeng *et al.* [21] developed a compositional method to model the dependent behaviors among failure mechanisms, by combining physics-of-failure models of the individual mechanisms and models of interactions among the mechanisms.

Most of the existing works on DCFP, as reviewed above, are limited to offline analysis, assuming that the model parameters are known *a priori* and fixed during the entire life cycle of the system. There are two major shortcomings for the offline analysis methods: first, to estimate the parameters *a priori*, large amount of empirical data are needed, which is, seldom fulfilled in engineering practices; and second, the offline analysis fails to capture any time dependence in the processes. On the other hand, nowadays, the advancement of sensor systems [22] has enabled condition monitoring and data on the degradation processes of mechanical equipment and electronic devices have been made available for system reliability assessment. With condition-monitoring data, system reliability, and remaining useful life (RUL) [23], [24] can be assessed online and predicted via data-driven or model-based approaches [25].

For DCFP, however, RUL prediction is challenging because dependencies exist among failure processes and shocks are hard to observe in practice. This is why only a few works in literature focus on RUL prediction in presence of DCFP. Wang *et al.* [26] developed a prognostics framework for DCFP based on particle filtering (PF), considering soft failures caused by degradation, and hard failures resulting from random shocks. Ke *et al.* [27] investigated RUL prediction for a nonstationary degradation process with random shocks; a modified Kalman filter model was developed to estimate the system hidden degradation state and the degradation model parameters were estimated by maximum likelihood estimation with the expectation maximization algorithm; to apply the model, the shock arrival time must be known. Zhang *et al.* [28] considered a system subject to degradation and time-varying random jumps, and developed an approximated analytical solution for the predicted lifetime, where a two-step expectation conditional maximization algorithm was used for estimating model parameters.

In the existing methods, it is assumed that system failure can only be caused by the degradation process. In practice, however, hard failure can also be caused by random shocks. Besides, existing methods are based on a strict assumption that the arrival time of the shocks need to be observed [27]. To overcome these limitations, we propose a new sequential Bayesian approach for RUL prediction in presence of DCFP. Compared to the existing methods, the main originalities of the proposed method are as follows.

1) Hard failures are also considered for the RUL prediction of DCFP.
2) Estimation of the parameters of the shock process is properly addressed.

The remainder of this paper is organized as follows. Section II defines the DCFP model considered in this paper. In Section III, a sequential Bayesian approach for RUL prediction is developed. In Section IV, the performance of the developed method is compared to existing methods through two numerical examples. Then, the developed method is applied to a real case study of a milling machine in Section V. Finally, the paper is concluded with some discussion on the future work in Section VI.

II. System Description

For illustrative purposes, we consider a DCFP model adapted from literature [4], which comprises a degradation process $x(t)$ and a random shock process ($W(t)$) with dependencies. The random shocks are further divided based on their magnitudes: a fatal shock (the shock with a magnitude greater than a critical level D) directly fails the system, while a nonfatal shock (the shock with a magnitude less than the critical level D) brings an additional damage S to the degradation process $x(t)$, as shown in Fig. 1 [4].

Assumptions of the DCFP model include the following.

1) The continuous degradation process follows a Brownian motion with a linear drift

$$x\left(t\right)=\varphi+\eta t+\sigma_{x}B\left(t\right) \tag{1}$$

where η is the degradation rate, φ denotes the initial degradation level, assumed to be zero in this paper, $B(t)$ is the standard Brownian motion: $B(t)\sim \text{Normal}(0,t)$, and σ_x is the drift coefficient.

2) The arrival of the random shocks follows a homogenous Poisson process (HPP) with a constant intensity λ.

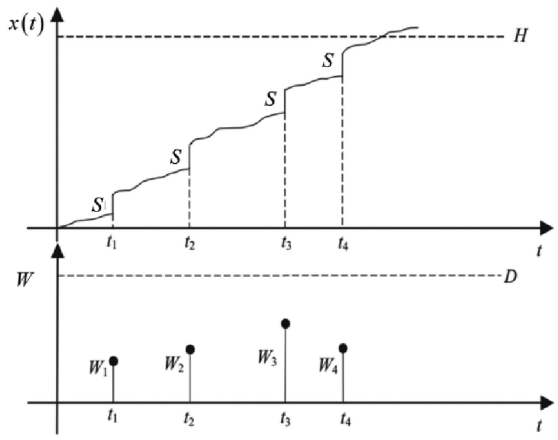

Fig. 1. DCFP model considered in this paper [4].

3) The magnitudes of the arrived shocks, denoted by W_i, follow *i.i.d.* normal distributions $W_i \sim \text{Normal}(\mu_W, \sigma_W^2)$ $i = 1, 2, \ldots$.
4) Each nonfatal shock (*i.e.*, $W_i < D$) brings an increment $S > 0$ to the degradation process $x(t)$.
5) Failures occur whenever one of the following two events occurs:
   a) the degradation process reaches the threshold H (soft failure);
   b) a fatal shock occurs (hard failure).
6) Condition-monitoring data $y_{1:k} = \{y_i, i = 1, \ldots, k\}$ are collected periodically at $t = t_1, \ldots, t_k$, where $t_k - t_{k-1} = t_{k-1} - t_{k-2} = \cdots = t_2 - t_1 = \tau$ and y_i is the degradation measurement at $t = t_i$

$$y_i = z(t_i) + \epsilon_y \tag{2}$$

where $\epsilon_y \sim \text{Normal}(0, \sigma_y^2)$ is the observation noise; $z(t_i)$ is the overall degradation considering both the continuous degradation process and the abrupt change brought by the random shocks

$$z(t_i) = x(t_i) + \sum_{j=1}^{N(t_i)} I(W_j < D) \cdot S \tag{3}$$

where $N(t_i)$ denotes the number of arrival shocks prior to t_i, $I(\cdot)$ is the indicator function and is defined by

$$I(A) = \begin{cases} 1, & \text{if A is true} \\ 0, & \text{if A is false.} \end{cases} \tag{4}$$

7) At most one shock can arrive in the inspection interval $(t_{i-1}, t_i], i = 2, \ldots, k$.

III. Developed Methods

In this section, we present the developed approach for RUL prediction of the DCFP. A state-space model is developed in Section III-A to describe the DCFP. A sequential Bayesian approach is developed in Section III-B, C, and D to update the estimated parameter values of the state-space model based on the newly collected observation data. The RUL of the DCFP is, then, predicted in Section III-E using the updated parameter values.

A. State-Space Model for the DCFP

Let $\theta_k = [z_k, \eta_k, S_k, \lambda_k]$ denote the values of state variables for the DCFP model at $t = t_k$. The state-space model for the DCFP comprises of a process model, which describes how the state variables evolve over time, and an observation model that relates the state variables to the observation data y_k

$$\begin{cases} \theta_k = h(\theta_{k-1}) + \omega, & \text{(Process model)} \\ y_k = g(\theta_k) + \nu, & \text{(Observation model)} \end{cases} \tag{5}$$

where ω and ν are the process and observation noises, respectively.

In this paper, we assume that η and S are subject to process noises resulting from environmental and operation conditions. Therefore, the time-varying process models for η and S are assumed to be

$$\eta_k = \eta_{k-1} + \omega_\eta \tag{6}$$

$$S_k = S_{k-1} + \omega_S \tag{7}$$

where $\omega_\eta \sim \text{Normal}(0, \sigma_\eta^2)$ and $\omega_S \sim \text{Normal}(0, \sigma_S^2)$ are the process noises for η and S, respectively. On the other hand, we assume that the state variable λ is a constant (but unknown) value, as by its definition, the intensity of an HPP is a constant value over the given time horizon. Therefore, the process model for λ is

$$\lambda_k = \lambda_{k-1} = \cdots = \lambda_0. \tag{8}$$

Based on assumption (2), the number of shocks arrived prior to t, denoted by $N(t; \lambda_0)$, follows the Poisson distribution

$$\Pr\{N(t; \lambda_0) = n\} = \frac{(\lambda_0 t)^n \cdot \exp(\lambda_0 t)}{n!}, n \in \mathbb{N}. \tag{9}$$

Let p_f denote the probability that a shock is a fatal shock and p_d the probability that it is a nonfatal shock. According to assumptions (3) and (4), p_f and p_d are

$$p_f = 1 - \Phi\left(\frac{D - \mu_W}{\sigma_W}\right), p_d = \Phi\left(\frac{D - \mu_W}{\sigma_W}\right) \tag{10}$$

where $\Phi(\cdot)$ is the cumulative distribution function (CDF) of the standard normal distribution. Then, according to [29], the shock process can be further split into two independent HPPs: a fatal shock process $\{N_f(t; \lambda_f)\}$ and a nonfatal shock process $\{N_d(t; \lambda_d)\}$, where λ_f, λ_d are the intensities of the fatal shock process and the nonfatal shock process and $\lambda_f = p_f \lambda_0, \lambda_d = p_d \lambda_0$, respectively.

Then, considering the continuous degradation process defined by assumption (1) and the dependency defined by assumption (4), the process model for z_k can be derived

$$z_k = z_{k-1} + \tau \cdot \eta_k + S_k \cdot I(N(t; p_d \lambda_k) = 1) + \omega_z \tag{11}$$

where τ is the data collection interval defined in assumption (6). From (3), the process noise $\omega_z \sim \text{Normal}(0, \sigma_x^2 \tau)$.

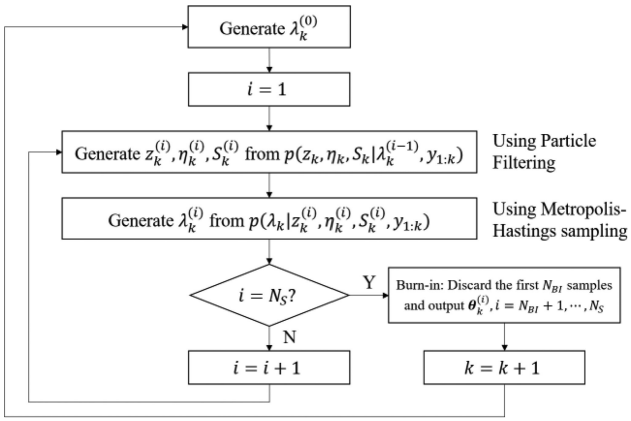

Fig. 2. Hybrid Gibbs-MH algorithm for parameter estimation at $t = t_k$.

The observation model for the DCFP can be easily derived from (2)

$$\begin{aligned} y_k &= g(\theta_k) + \nu \\ &= z_k + \epsilon_y \end{aligned} \tag{12}$$

where the observation noise $\nu = \epsilon_y \sim \text{Normal}(0, \sigma_y^2)$.

B. Sequential Bayesian Framework for Parameter Estimation

Based on the developed state-space model in (6)–(12), a sequential Bayesian framework can be developed to update the estimated model parameter θ at $t = t_i, i = 1, 2, \ldots, k$, using the observation data prior to t. Without losing generality, we illustrate the framework at $t = t_k$. According to Bayes' theorem, the posterior probability density of θ_k can be calculated by

$$\begin{aligned} p(\theta_k|y_{1:k}) &= p(z_k, \eta_k, S_k, \lambda_k|y_{1:k}) \\ &= \frac{p(y_{1:k}|z_k, \eta_k, S_k, \lambda_k) \cdot p(z_k, \eta_k, S_k, \lambda_k)}{p(y_{1:k})}. \end{aligned} \tag{13}$$

Directly solving (13) is often computationally intractable due to the complexity in the involved distributions. A hybrid Gibbs—Metropolis–Hastings (MH) algorithm is, therefore, developed in Fig. 2, to generate N_S samples $\theta_k^{(i)} = [z_k^{(i)}, \eta_k^{(i)}, S_k^{(i)}, \lambda_k^{(i)}], i = 1, 2, \ldots, N_S$ to approximate the posterior distribution of θ_k. The algorithm comprises two iterative steps: in the first step, samples for $z_k^{(i)}, \eta_k^{(i)}, S_k^{(i)}$ are generated from the conditional distribution $p(z_k, \eta_k, S_k|\lambda_k^{(i-1)}, y_{1:k})$. In this paper, as the explicit form of $p(z_k, \eta_k, S_k|\lambda_k^{(i-1)}, y_{1:k})$ is too complex to be derived, we generate $z_k^{(i)}, \eta_k^{(i)}, S_k^{(i)}$ recursively, using particle filtering (see Section III-C). Then, in the second step, MH sampling is used to generate a sample $\lambda_k^{(i)}$ from the conditional distribution $p(\lambda_k|z_k^{(i)}, \eta_k^{(i)}, S_k^{(i)}, y_{1:k})$ (see Section III-D). It can be shown that following the algorithm in Fig. 2, the generated $\theta_k^{(i)}, i = 1, 2, \ldots, N_S$ comprise a Markov chain whose stationary distribution is $p(\theta_k|y_{1:k})$ [30]. Therefore, after a large number of iterations, the generated sequence $\theta_k^{(i)}, i = N_{BI} + 1, 2, \ldots, N_S$ converges to samples from the posterior distribution of the model parameters. It should be noted that in practice, the first N_{BI} samples in the generated sequence are often discarded for burn-in purposes, to ensure that the simulated Markov chain enters the stationary period and that the generated samples come from the stationary distribution of the Markov chain.

C. Updating Degradation Parameters Using PF

As shown in Fig. 2, PF is used to generate $z_k^{(i)}, \eta_k^{(i)}, S_k^{(i)}$ from the conditional distribution $p(z_k, \eta_k, S_k|\lambda_k^{(i-1)}, y_{1:k})$. PF is used, in this paper, for its capability to handle the nonlinearity of degradation processes for degradation state estimation [31]–[34]. Conditioning on $\lambda_k^{(i-1)}$, the state-space model for the DCFP reduces to (14), shown at the bottom of this page, where $\omega_\eta, \omega_S, \omega_z$, and ν are process noises and observation noise that are defined in (6), (7), (11), and (12), respectively; $\lambda_k^{(i-1)}$ is obtained from MH sampling in the second step of the algorithm.

Let $\mathbf{J}_k = [z_k, \eta_k, S_k]$; in PF, the posterior density of $\mathbf{J}_k$, denoted by $p(\mathbf{J}_k|y_{1:k}, \lambda_k^{(i-1)})$, is recursively estimated based on Bayes' theorem [31], [35]:

$$p(\mathbf{J}_k|y_{1:k}) = \frac{p(y_k|\mathbf{J}_k)\, p(\mathbf{J}_k|y_{1:k-1})}{\int p(y_k|\mathbf{J}_k)\, p(\mathbf{J}_k|y_{1:k-1})\, d\mathbf{J}_k}. \tag{15}$$

It should be noted that for simplicity of presentation and without causing ambiguity, we drop $\lambda_k^{(i-1)}$ in the conditional probabilities in (15) and also in the remaining part of this section. In (15), $p(y_k|\mathbf{J}_k)$ is determined by the observation model in (14) and $p(\mathbf{J}_k|y_{1:k-1})$ is obtained by (16)

$$p(\mathbf{J}_k|y_{1:k-1}) = \int p(\mathbf{J}_k|\mathbf{J}_{k-1})\, p(\mathbf{J}_{k-1}|y_{1:k-1})\, d\mathbf{J}_{k-1} \tag{16}$$

where $p(\mathbf{J}_k|\mathbf{J}_{k-1})$ is determined by the process model in (14) and $p(\mathbf{J}_{k-1}|y_{1:k-1})$ is obtained by the output of the PF at $t = t_{k-1}$.

In PF, (15) is approximated by a sequential importance sampling algorithm [31], where the posterior density $p(\mathbf{J}_k|y_{1:k})$ is approximated by a set of random samples (called particles) with associated weights, denoted by $\{\mathbf{J}_k^{(j)}, w_k^{(j)}\}, j = 1, \ldots, M$

$$p(\mathbf{J}_k|y_{1:k}) \approx \sum_{j=1}^{M} w_k^{(j)} \delta\left(\mathbf{J}_k - \mathbf{J}_k^{(j)}\right) \tag{17}$$

$$\begin{cases} \begin{pmatrix} z_k \\ \eta_k \\ S_k \end{pmatrix} = \begin{pmatrix} z_{k-1} + \eta_{k-1} \cdot \tau + S_{k-1} \cdot I\left(N\left(\tau; p_d \lambda_k^{(i-1)}\right) = 1\right) \\ \eta_{k-1} \\ S_{k-1} \end{pmatrix} + \begin{pmatrix} \omega_z \\ \omega_\eta \\ \omega_S \end{pmatrix} \\ y_k = z_k + \nu \end{cases} \tag{14}$$

Algorithm 1: Generate $z_k^{(i)}, \eta_k^{(i)}, S_k^{(i)}$ using PF.

Inputs: $\{\mathbf{J}_{k-1}^{(j)}, w_{k-1}^{(j)}, j = 1, \ldots, M\}, y_k$ $\frac{1}{2}$
Outputs: $z_k^{(i)}, \eta_k^{(i)}, S_k^{(i)}$
1: **for** $j = 1{:}\, M$ **do**
2: Sample $\mathbf{J}_k^{(j)}$ by (18);
3: **end for**
4: Update $w_k^{(j)}, j = 1, 2, \ldots, M$, by (19);
5: $N_{eff} = (\sum_{i=1}^{M} (w_k^j)^2)^{-1}$;
6: **if** $N_{eff} < M/2$ **then**
7: Resampling using the systematic resampling algorithm [31]
8: **end if**
9: $z_k^{(i)}, \eta_k^{(i)}, S_k^{(i)} \leftarrow$ Draw a sample from $\{\mathbf{J}_k^{(j)}\}$, where $\Pr(\mathbf{J}_k^{(j)}$ is selected$) = w_k^{(j)}$

where $\delta(\cdot)$ is the Dirac delta function. In this paper, at each time $t = t_k$, the particles are generated from a proposal density $p(\mathbf{J}_k|\mathbf{J}_{k-1})$

$$\mathbf{J}_k^{(j)} \sim p\left(\mathbf{J}_k \left|\mathbf{J}_{k-1}\right.\right). \tag{18}$$

Then, the associated weights $w_k^{(j)}$ are updated by [31]

$$w_k^{(j)} = \frac{w_{k-1}^{(j)} p\left(y_k \left|\mathbf{J}_k^{(j)}\right.\right)}{\sum_{i=1}^{M} w_{k-1}^{(j)} p\left(y_k \left|\mathbf{J}_k^{(j)}\right.\right)}. \tag{19}$$

Since $\{\mathbf{J}_k^{(j)}, w_k^{(j)}\}, j = 1, \ldots, M$ approximate the required conditional posterior density through (17), $z_k^{(i)}, \eta_k^{(i)}, S_k^{(i)}$ can be generated by drawing one sample from $\{\mathbf{J}_k^{(j)}\}, j = 1, 2, \ldots, M$ where the probability of drawing the jth particle $\mathbf{J}_k^{(j)}$ is $w_k^{(j)}$. The algorithm for generating $z_k^{(i)}, \eta_k^{(i)}, S_k^{(i)}$ is summarized in Algorithm 1.

D. Updating Shock Intensity Using MH Sampling

MH algorithm [30] is used to generate $\lambda_k^{(i)}$ from the conditional posterior distribution $p(\lambda_k|z_k^{(i)}, \eta_k^{(i)}, S_k^{(i)}, y_{1:k})$. It should be noted that apart from the condition-monitoring data $y_{1:k}$, system operation time t_k can also be used to update the posterior distribution, as it implies that no fatal shock occurs prior to t_k: $N_f(t_k) = 0$ (otherwise the system should have failed before t_k). For simplicity of presentation and without causing ambiguity, we drop the $z_k^{(i)}, \eta_k^{(i)}, S_k^{(i)}$ in the conditional probability and denote it by $p(\lambda_k|y_{1:k}, N_f(t_k) = 0)$ in the remaining part of this section.

From Bayes' theorem, the posterior density is derived as

$$\begin{aligned} &p\left(\lambda_k|y_{1:k}, N_f\left(t_k\right) = 0\right) \\ &\propto p\left(y_{1:k}, N_f\left(t_k\right) = 0|\lambda_k\right) p\left(\lambda_k\right) \\ &= p\left(y_{1:k}|\lambda_k\right) \cdot p\left(N_f\left(t_k\right) = 0|\lambda_k\right) \cdot p\left(\lambda_k\right) \end{aligned} \tag{20}$$

where the prior distribution $p(\lambda_k)$ is assumed to be a uniform distribution Uniform$(\underline{\lambda}, \bar{\lambda})$ in this paper, and $p(N_f(t_k) = 0|\lambda_k)$ is calculated by

$$p\left(N_f\left(t_k\right) = 0|\lambda_k\right) = e^{-\lambda_k \cdot p_f \cdot t_k} \tag{21}$$

where p_f is calculated by (10).

To simplify the computation of $p(y_{1:k}|\lambda_k)$, we neglect the observation noise ν and the process noise ω_η, ω_S in the state-space model (14). Therefore, $p(y_{1:k}|\lambda_k)$ can be approximated by (22), where $\varphi(\cdot)$ is the standard normal density function; σ_x is the process noise of the degradation levels defined in (14); $\eta_k^{(i)}$ and $S_k^{(i)}$ are the MCMC samples generated from the first step in Fig. 2. It should be noted that in (22), $p(z_i|z_{i-1})$ is determined by the process model defined in (11)

$$\begin{aligned} &p\left(y_{1:k}\left|\lambda_k\right.\right) = p\left(z_{1:k}\left|\lambda_k\right.\right) \\ &= p\left(z_1\left|z_0\right.\right) \cdot \prod\nolimits_{j=2}^{k} p\left(z_j\left|z_{j-1}, \lambda_k\right.\right) \\ &= p\left(z_1\left|z_0\right.\right) \cdot \prod\nolimits_{j=2}^{k} \\ &\quad \times \begin{pmatrix} p\left(z_j\left|z_{j-1}, N_d\left(\tau\right) = 1\right.\right) \cdot \Pr\left(N_d\left(\tau\right) = 1\right) \\ +p\left(z_j\left|z_{j-1}, N_d\left(\tau\right) = 0\right.\right) \cdot \Pr\left(N_d\left(\tau\right) = 0\right) \end{pmatrix} \\ &= \varphi\left(\frac{y_1}{\sigma_x}\right) \\ &\prod\nolimits_{j=2}^{k} \begin{pmatrix} \varphi\left(\frac{y_j - y_{j-1} - \eta_k^{(i)}\tau - S_k^{(i)}}{\sigma_x}\right) \cdot \left(p_d \lambda_k \tau\right) \cdot \exp\left(-p_d \lambda_k \tau\right) \\ +\varphi\left(\frac{y_j - y_{j-1} - \eta_k^{(i)}\tau}{\sigma_x}\right) \cdot \exp\left(-p_d \lambda_k \tau\right) \end{pmatrix}. \end{aligned} \tag{22}$$

The MH algorithm generate samples from the posterior distribution in an iterative way: in each iteration j, a candidate point λ_k^* is first generated from a proposal density $g(\cdot)$. In this paper, we use the prior distribution Uniform$(\underline{\lambda}, \bar{\lambda})$ as the proposal density. Then, the acceptance probability, denoted by r, is calculated by

$$\begin{aligned} r &= \min\left(1, \frac{p\left(\lambda_k^*\left|y_{1:k}, N_f\left(t_k\right) = 0\right.\right)}{p\left(\lambda_k^{(j-1)}\left|y_{1:k}, N_f\left(t_k\right) = 0\right.\right)} \cdot \frac{g\left(\lambda_k^{(j-1)}\left|\lambda_k^*\right.\right)}{g\left(\lambda_k^*\left|\lambda_k^{(j-1)}\right.\right)}\right) \\ &= \min\left(1, \frac{p\left(y_{1:k}\left|\lambda_k^*\right.\right) \cdot p\left(N_f\left(t_k\right) = 0\left|\lambda_k^*\right.\right)}{p\left(y_{1:k}\left|\lambda_k^{(j-1)}\right.\right) \cdot p\left(N_f\left(t_k\right) = 0\left|\lambda_k^{(j-1)}\right.\right)}\right). \end{aligned} \tag{23}$$

The candidate point is accepted with probability r and rejected with probability $(1 - r)$. This process is repeated until enough samples are generated to approximate the posterior density. Usually, it takes the MCMC algorithm several iterations to converge to the stationary distribution. For a more accurate approximation of the posterior density, a "burn-in" stage is conducted to exclude samples from the beginning of the MCMC, which are far away from the stationary distribution [36]. It should be noted that for systems not influenced by hard failures, like those in [27] and [28], generally no catastrophic

Algorithm 2: Generate $\lambda_k^{(i)}$ using MCMC [30].

Inputs: $\underline{\lambda}, \bar{\lambda}, \mathbf{J}_k^{(i)}, y_{1:k}, t_k$
Outputs: $\lambda_k^{(i)}$
1: Sample λ_k^* from $Uniform(\underline{\lambda}, \bar{\lambda})$;
2: Compute r by (23);
3: Sample u from $Uniform(0,1)$;
4: **if** $u \leq r$ **then**
5: Set $\lambda_k^{(i)} = \lambda_k^*$;
6: **else**
7: Set $\lambda_k^{(i)} = \lambda_k^{(i-1)}$;
8: **end if**

shock strikes the system and (23) can be simplified to

$$r = \min\left(1, \frac{p\left(y_{1:k}\,|\lambda_k^*\right)}{p\left(y_{1:k}\,\middle|\lambda_k^{(j-1)}\right)}\right). \tag{24}$$

A summary of the MH algorithm is given by Algorithm 2.

E. RUL Prediction

Using the algorithm developed in Fig. 2, N_S samples $\theta_k^{(i)} = [z_k^{(i)}, \eta_k^{(i)}, S_k^{(i)}, \lambda_k^{(i)}], i = 1, 2, \ldots, N_S$ can be generated to approximate the posterior distribution $p(\theta|y_{1:k})$ at $t = t_k$. The distribution of RUL can, then, be predicted based on these samples.

Since in the DCFP model of Section II, hard failures are random, the RUL should be predicted in terms of its probability density function. Let RUL_k denote the predicted RUL at $t = t_k$ and TTF_k denote the updated time-to-failure at $t = t_k$. It can be seen that RUL_k is a conditional random variable [37] in the form of $\mathrm{RUL}_k = (\mathrm{TTF}_k - t_k|\mathrm{TTF}_k > t_k)$, which defines the remaining lifetime of the system given that it has survived up to time t_k, and

$$\begin{aligned}&(\mathrm{TTF}_k\,|\mathrm{TTF}_k > t_k\,)\\ &= \min\left\{(\mathrm{TTSF}\,|y_{1:k}, \mathrm{TTSF} > t_k\,), (\mathrm{TTHF}\,|\mathrm{TTHF} > t_k\,)\right\}\end{aligned} \tag{25}$$

where TTSF and TTHF represent the time to soft failure and time to hard failure, respectively.

In (25), the conditional random variable $(\mathrm{TTSF}|y_{1:k}, \mathrm{TTSF} > t_k)$ is derived by the first passage time of the degradation process

$$\begin{aligned}(\mathrm{TTSF}|\,y_{1:k}, \mathrm{TTSF} > t_k) = \inf\{t_{k+l} : z_{k+l}\\ \geq H|z_k, z_k < H\}\end{aligned} \tag{26}$$

where z_{k+l} is predicted according to (14).

From Assumption (2), the hard failure process is a Poisson process with a rate parameter $p_f\lambda$. Therefore, TTHF is a random variable following an exponential distribution with rate $p_f\lambda_k$, *i.e.*, $\mathrm{TTHF} \sim \exp(p_f\lambda_k)$. The CDF of $\mathrm{TTHF}|\mathrm{TTHF} > t_k$ can, then, be calculated

$$\begin{aligned}P\left(\mathrm{TTHF} \leq t\,|\mathrm{TTHF} > t_k\,\right) &= \frac{P\left(t_k < \mathrm{TTHF} \leq t\right)}{P\left(\mathrm{TTHF} > t_k\right)}\\ &= 1 - \exp\left(-p_f\lambda_k\left(t - t_k\right)\right).\end{aligned} \tag{27}$$

Therefore, we have

$$\left(\mathrm{TTHF} - t_k\,|\mathrm{TTHF} > t_k\,\right) \sim \exp\left(p_f\lambda_k\right). \tag{28}$$

The distribution of RUL_k can, then, be derived by substituting (28) and (26) into (25). In this paper, due to the complexities in (26) and (28), we develop a simulation-based method for RUL prediction, as shown in Algorithm 3.

Algorithm 3: Algorithm for RUL Estimation.

Inputs: $\theta_k^{(i)} = [z_k^{(i)}, \eta_k^{(i)}, S_k^{(i)}, \lambda_k^{(i)}], i = 1, 2, \ldots, N_S$
Outputs: $\{RUL_k^{(j)}, j = 1, \ldots, N_s\}$
1: **for** $j = 1 : N_s$ **do**
2: $l = 1$;
3: **while 1 do**
4: Calculate $z_{k+l}^{(j)}$ by (14) with $\theta = \theta_k^{(j)}$
5: **if** $z_{k+l} \geq H$ **then**
6: $RUL_{S,k}^{(j)} = l$; **break**
7: **else**
8: $l = l + 1$;
9: **end if**
10: **end while**
11: Sample $\mathrm{RUL}_{H,k}^{(j)}$ from $\exp(p_f\lambda_k^{(j)})$
12: $\mathrm{RUL}_k^{(j)} = \min(\mathrm{RUL}_{S,k}^{(j)}, \mathrm{RUL}_{H,k}^{(j)})$;
13: **end for**

It should be noted that Algorithm 3 also applies for DCFPs in which only soft failures lead to system failures: in these cases, $\mathrm{RUL}_{H,k}$ is not considered and system RUL is only determined by $\mathrm{RUL}_{S,k}$.

IV. Numerical Example

A similar RUL prediction method has been developed by Ke *et al.* [27] for the DCFPs considered in this paper. In this section, the performances of the two methods are compared through two numerical examples. In Section IV-A, the numerical case from [27] is directly used to test the developed method, where the dependency between shocks and degradations are considered without further considering the possibility of hard failures. Then, in Section IV-B, a more complete model involving hard failures is considered.

A. Example 1

A system subject to degradation and nonfatal shocks is considered in this numerical example. The system failure process is the same as that in Section II, except that, in this case, we do not consider hard failures. Therefore, we have $p_f = 0$. Degradation data and shock arrival time data (required by Ke's method [27])

TABLE I
TRUE VALUES OF PARAMETERS USED TO GENERATE SIMULATION DATA

Parameter	Description	True value
η_0	Degradation rate	0.5
S_0	Shock damage	0.5
λ_0	Shock intensity	0.53
τ	Testing period	0.2
σ_x^2	Diffusion coefficient of the standard Brown motion	0.05
H	Threshold for soft failure	53.63
N_M	The number of measurement points	500

TABLE II
PARAMETERS FOR SIMULATION WITH THE DEVELOPED METHOD

Parameter	Value	Parameter	Value
σ_x^2	0.05	σ_y^2	1×10^{-2}
σ_η^2	1×10^{-4}	$\underline{\lambda}$	1×10^{-3}
σ_S^2	1×10^{-4}	$\overline{\lambda}$	1

are generated using Monte Carlo simulation with the parameters in Table I.

Both the developed method and Ke's method are applied to estimate the model parameters and predict the RUL based on the generated data. A major difference between the two methods is that Ke's method requires to observe the precise shock arrival time, which is hard to achieve in practice. In this example, we also test the performance of the two methods when the shock arrival time data are not precise. To do this, the shock arrival time data are recorded as a binary variable sequence $\{I_s(t_k), k = 1, \ldots, N_M\}$, where $I_s(t_k) = 1$ implies that a shock arrives in time interval $[t_{k-1}, t_k)$ and $I_s(t_k) = 0$ means that no shock arrives in the time interval. To generate the imprecise shock arrival time data, given an error rate q, a random number r is generated from Uniform$(0, 1)$ at each time point t_k: if $r < q$, $I_s(t_k)$ is replaced by the imprecise data $I_s^c(t_k) = 1 - I_s(t_k)$; otherwise, $I_s(t_k)$ takes the correct value.

In the developed method, the prior distributions for z, η, S are *Normal*(0, 0.05), *Uniform*(0.4, 0.6), and *Uniform*(0.4, 0.6), respectively. Parameters used in the state-space model are given in Table II. In this case, we set the sample sizes to be $M = 100, N_s = 500$. In general, the more samples we select, the more accurate the parameter estimation and RUL prediction are. The computational complexity of the developed method is proportional to $M \times N_S$. Therefore, tradeoffs need to be made to determine the optimal sample sizes.

The updated parameters z, η, S and the predicted system RUL from the developed method and Ke's method are compared in Figs. 3–5 and 8. Estimates of the shock intensity λ obtained from the developed model are shown in Fig. 7. For the results from the developed method, as shown in Fig. 4(a), Fig. 5(a), and Fig. 6, we show both the mean and 90% credibility interval of the posterior distribution, while for Ke's method, we only show the posterior mean as only the posterior mean is discussed in their paper.

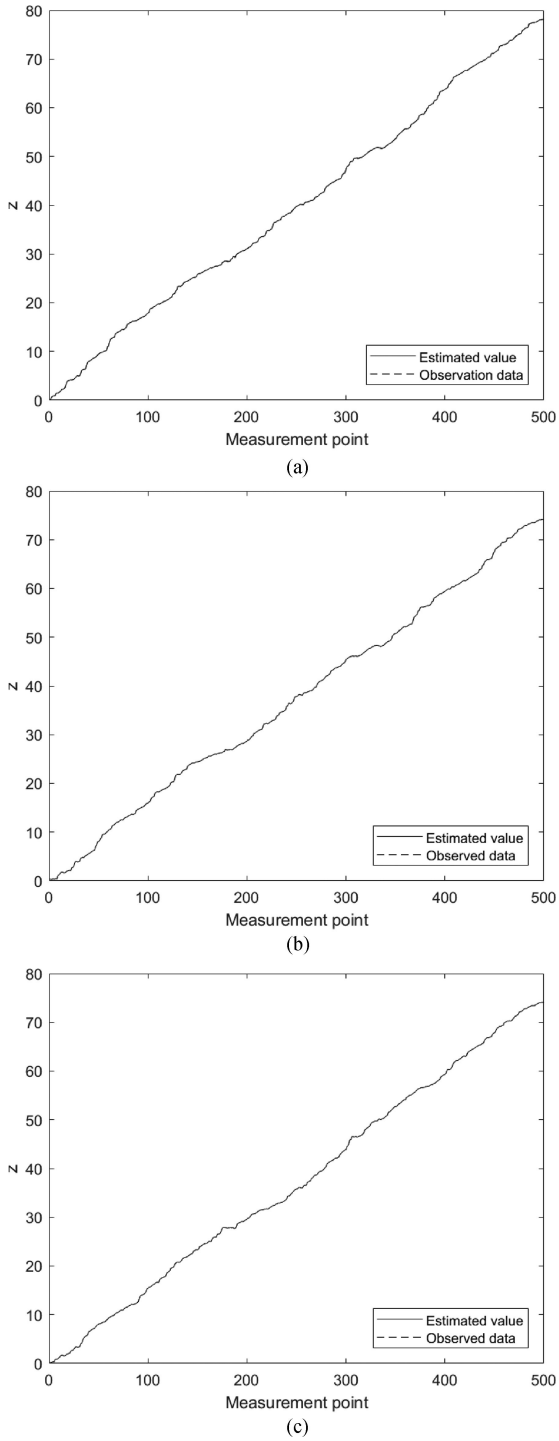

Fig. 3. Estimates of the degradation level. (a) Developed model. (b) Ke's model with accurate shock records. (c) Ke's model with imprecise shock records, error rate $q = 70\%$.

As shown in Fig. 3, both models produce accurate estimates of the system degradation level, given the observed degradation data. However, in Figs. 4, 5, and 8, it is shown that Ke's model can generate accurate estimates of the degradation model parameters and system RUL only if the shock arrival time are precisely observed. On the contrary, if the shock arrival times are imprecise (70% wrong data for example), Ke's method fails to provide

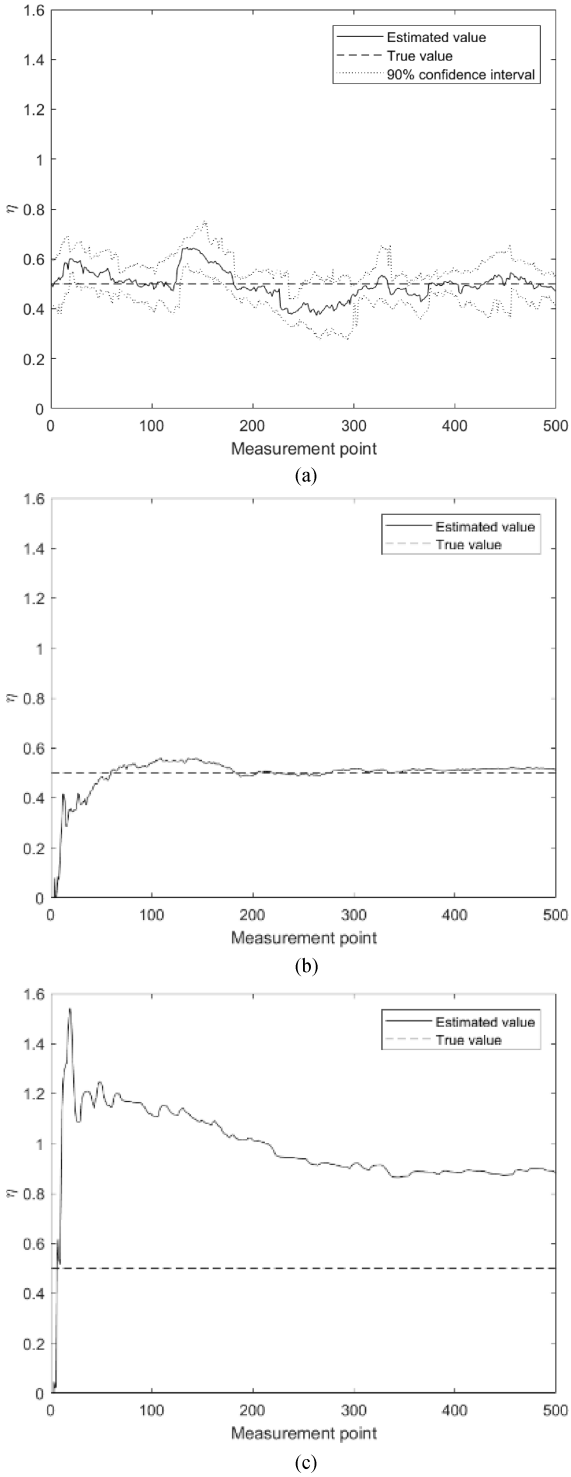

Fig. 4. Estimates of the degradation rate. (a) Developed model. (b) Ke's model with accurate shock records. (c) Ke's model with imprecise shock records, error rate $q = 70\%$.

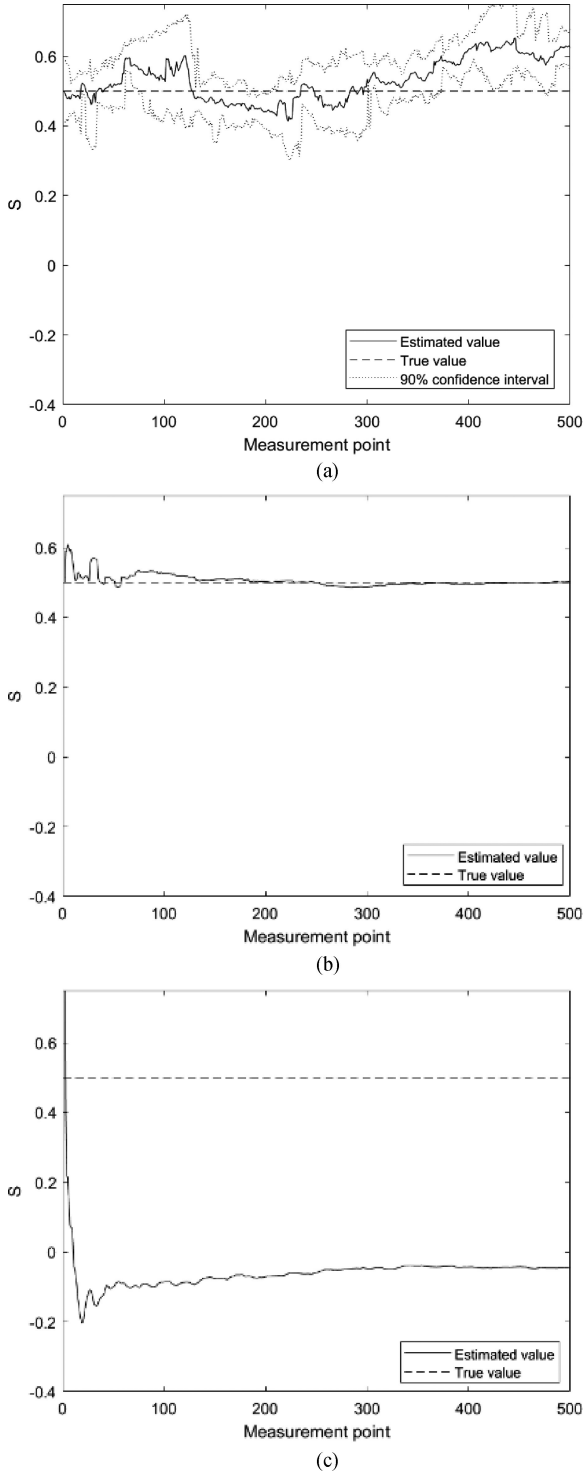

Fig. 5. Estimates of the shock damage. (a) The developed model. (b) Ke's model with accurate shock records. (c) Ke's model with imprecise shock records, error rate $q = 70\%$.

accurate parameters estimation and RUL prediction. The average error rates of parameter estimations with Ke's method in presence of imprecise shock data are listed in Table III. The results show that the accuracy of the estimation degrades as the increase of shock data error rate q.

On the other hand, Fig. 7 shows that the developed model performs well to estimate the shock intensity, without observing the arrival time of shocks. From the comparisons Figs. 4–8, it is shown that the developed model outperforms the Ke's method when observations of the shock arrival times are not precise,

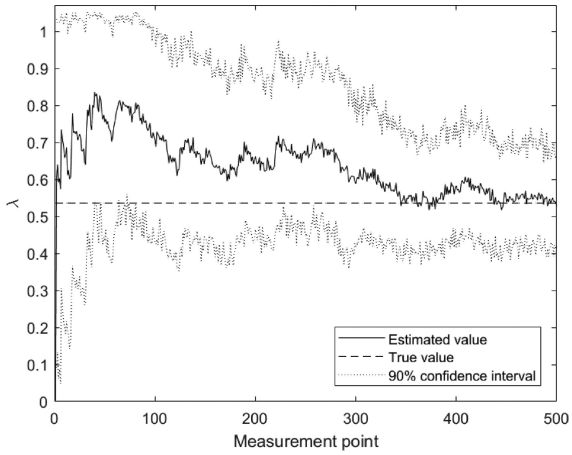

Fig. 6. Estimates of the shock intensity with the developed model.

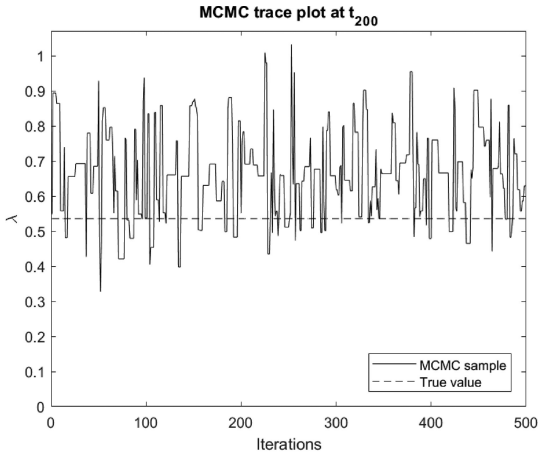

(a)

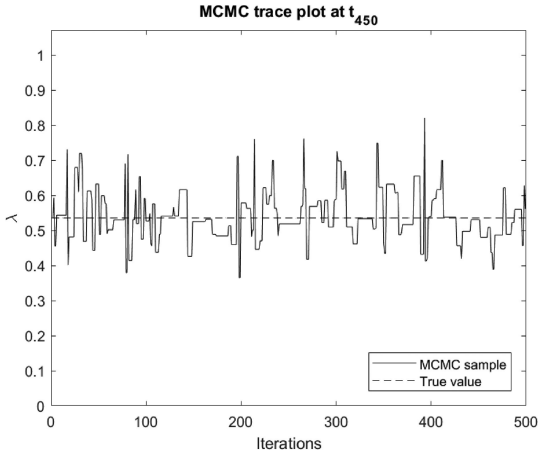

(b)

Fig. 7. Convergence analysis of the MCMC.

since the developed method does not require shock arrival data for parameter estimation and RUL prediction.

It should be noted that in the developed method, the convergence of the MCMC is monitored by checking the trace plots at each measurement point. For example, the trace plots for λ at $t = t_{200}$ and $t = t_{450}$ are shown in Fig. 7(a) and (b). It can

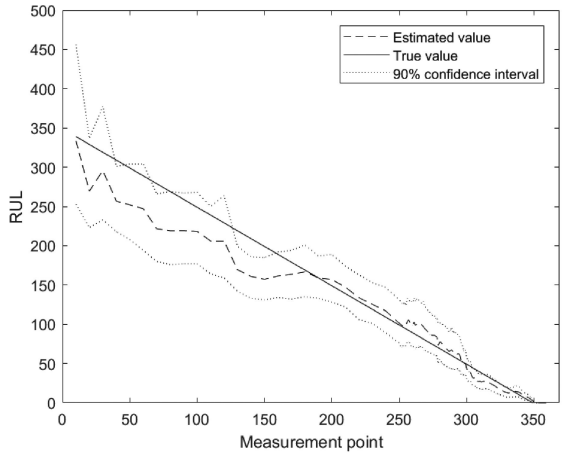

(a)

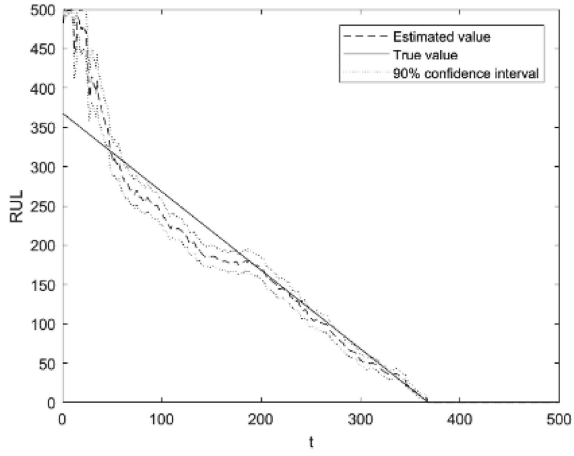

(b)

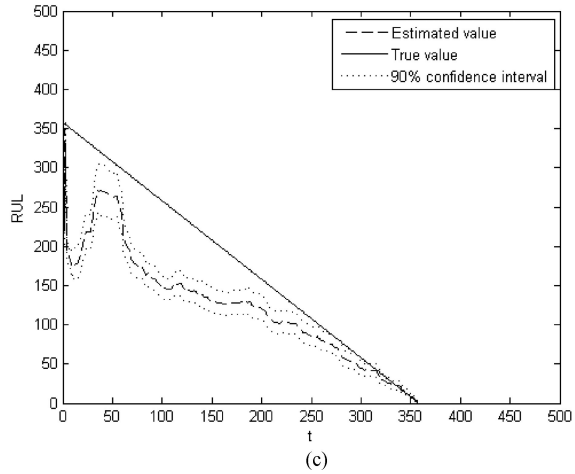

(c)

Fig. 8. Predicted RUL (a) the developed model; (b) Ke's model with accurate shock records; (c) Ke's model with imprecise shock records, error rate $q = 70\%$.

TABLE III
AVERAGE ERROR RATES OF PARAMETER ESTIMATIONS WITH KE'S METHOD IN PRESENCE OF IMPRECISE DATA

Error rate: q	$q = 0$	$q = 0.1$	$q = 0.3$	$q = 0.5$	$q = 0.7$
AER of estimated η	0.0682	0.1294	0.2972	0.7487	1.2403
AER of estimated S	0.0344	0.5107	0.8129	0.9791	1.1528

$AER = \sum_{k=1}^{N_M} \left| Estimation_k - True\ Value \right| \Big/ \left(True\ Value \cdot N_M \right)$

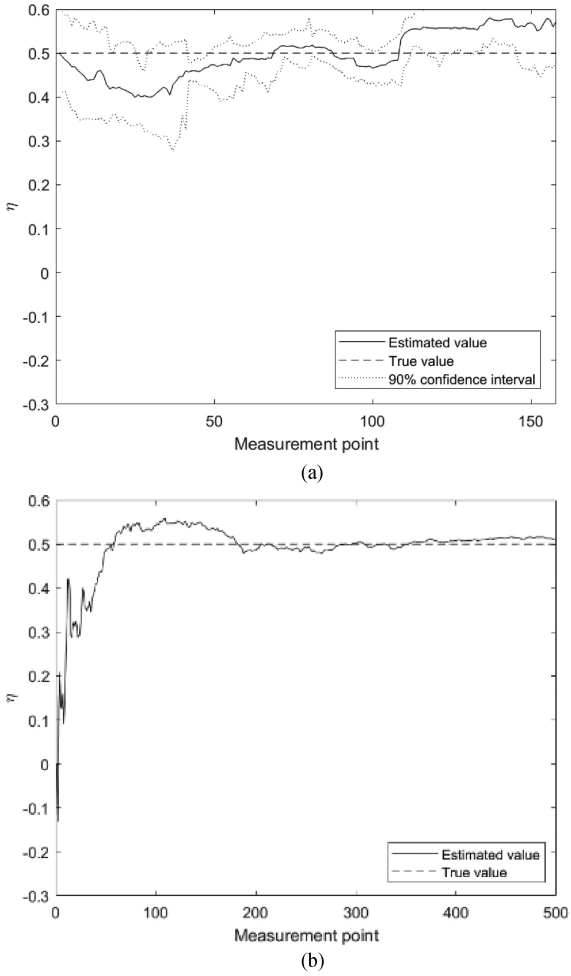

Fig. 9. Estimates of the degradation rate. (a) Developed model. (b) Ke's model.

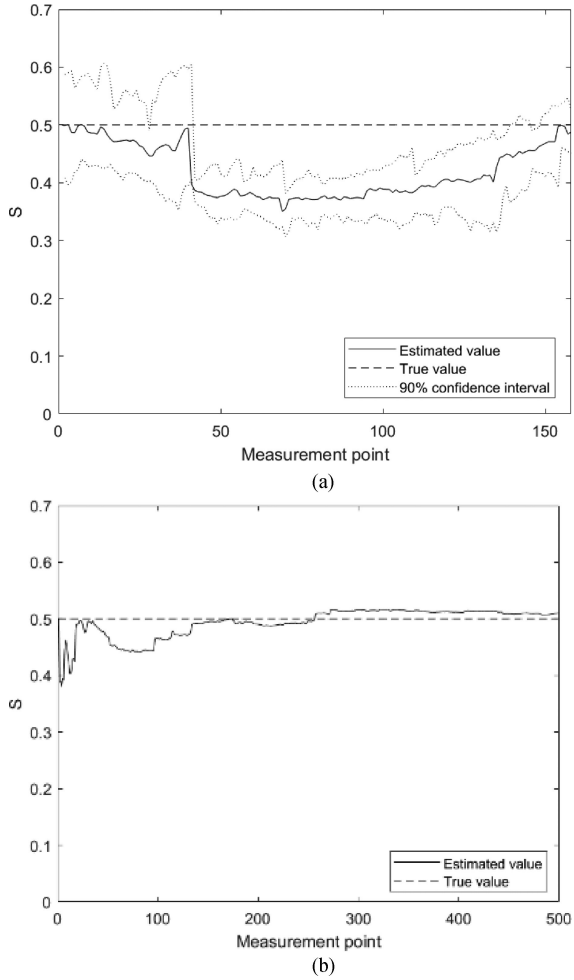

Fig. 10. Estimates of the shock damage. (a) Developed model. (b) Ke's model.

be seen from the figures that the MCMC samples converge to the true value. Further, as more and more degradation data are collected and used in the estimation of the shock intensity, the variance of the MCMC samples is significantly reduced.

B. Example 2

In this numerical example, the performance of the two methods previously considered is tested with respect to predicting RUL considering hard failures. The system defined in Section II is considered with $\mu_w = 1.2, \sigma_w = 0.2$ and $D = 1.5$. Then, p_f is calculated by (10). Using the parameters in Table I, degradation data and shock arrival time data are simulated. In this case, the simulated true TTF is t_{158}, which is due to a hard failure.

The same parameters as in Section IV-A are set for the implementation of the developed method. In this case, we set the sample sizes to be $M = 100, N_s = 500$. In general, the more samples we select, the more accurate the parameter estimation and RUL prediction are. The computational complexity of the developed method is proportional to $M \times N_S$. Therefore, tradeoffs need to be made to determine the optimal sample sizes.

The updated parameters η, S and predicted system RUL with the developed method and with Ke's method are compared in Figs. 9, 10, and 11. Estimates of the shock intensity λ obtained from the developed model are shown in Fig. 12. For the results from the developed method, we show the mean and 90% credibility interval of the posterior distribution, while for Ke's method, we only show the posterior mean as only the posterior mean is discussed in their paper.

As shown in Fig. 3 and 10, both models produce accurate estimates of the degradation rate η and the shock damage S. Fig. 12 shows that the developed model performs well to estimate the shock intensity, without observing the arrival time of shocks. However, in Fig. 11, it is shown that the PDF of system RUL is better predicted by the developed model than Ke's method, which yields an over-optimistic estimation of the RUL. The over-optimistic result of Ke's method is caused by the fact that it neglects the possibility of hard failures. In fact, in this case, the system fails at the early stage of its life cycle due to hard failure, even though the degradation level is still quite low and far less than the threshold of soft failures.

It should be noted that in the developed method, the convergence of the MCMC is monitored by checking the trace plots at each measurement point. For example, the trace plots for λ at $t = t_{50}$ and $t = t_{150}$ are shown in Fig. 13(a) and (b). It can be seen from the figures that the MCMC samples

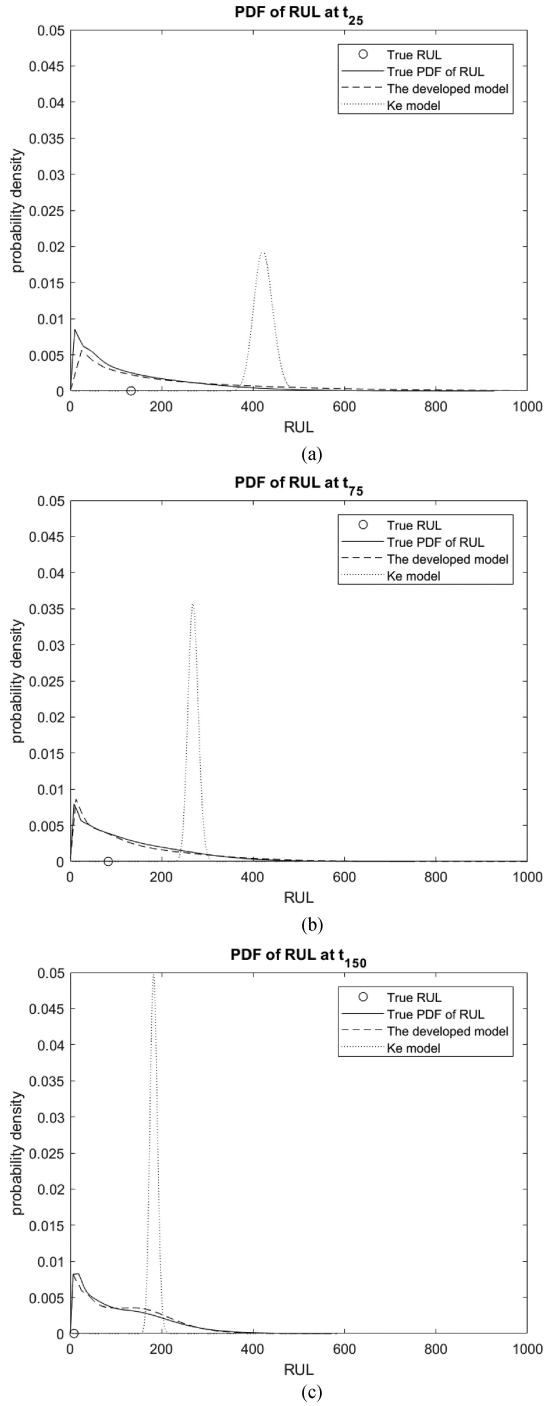

Fig. 11. Comparison of estimated RUL at (a) $t = t_{25}$; (b) $t = t_{75}$ and (c) $t = t_{150}$.

converge to the true value. Further, as more and more degradation data are collected and used in the estimation of the shock intensity, the variance of MCMC samples is significantly reduced.

V. Application

In this section, the developed model is applied on a real dataset of a milling machine from [38]. The original dataset contains

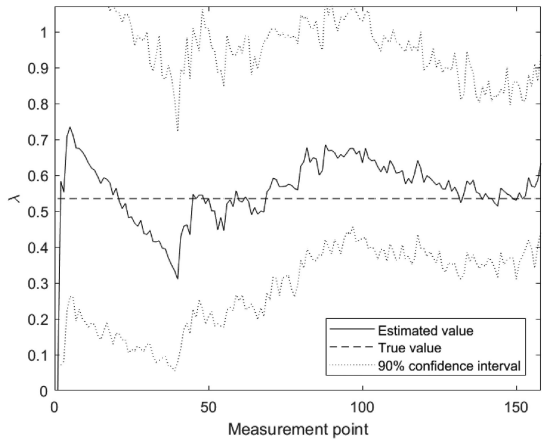

Fig. 12. Estimates of the shock intensity with the developed model.

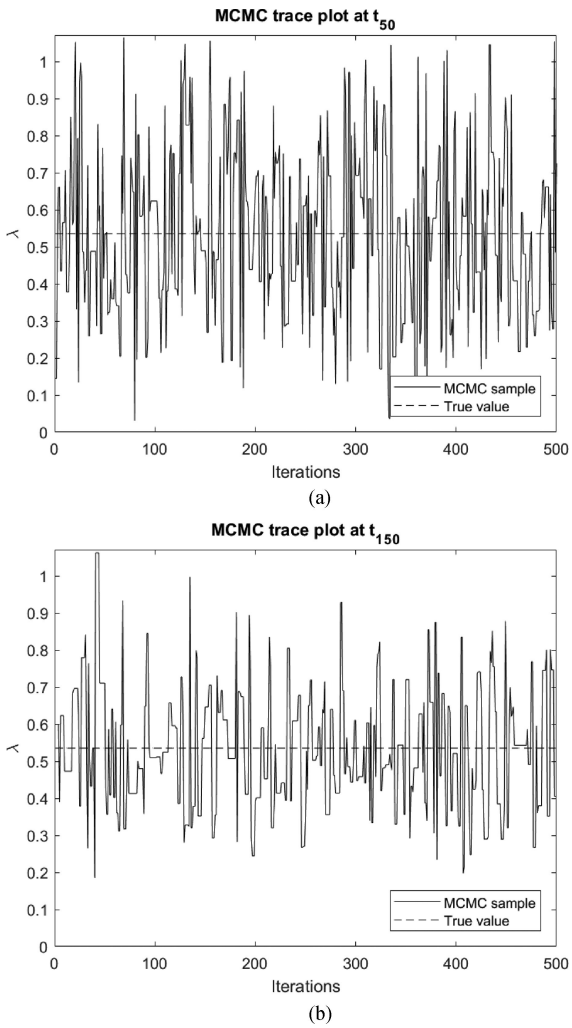

Fig. 13. Convergence analysis of the MCMC.

wear data of 16 different working conditions. The data from case 11 with 20 measurement points are used in this paper for state estimation and RUL prediction. As in [27], the threshold for soft failure is set to 0.42. No hard failure data are considered in the milling machine case.

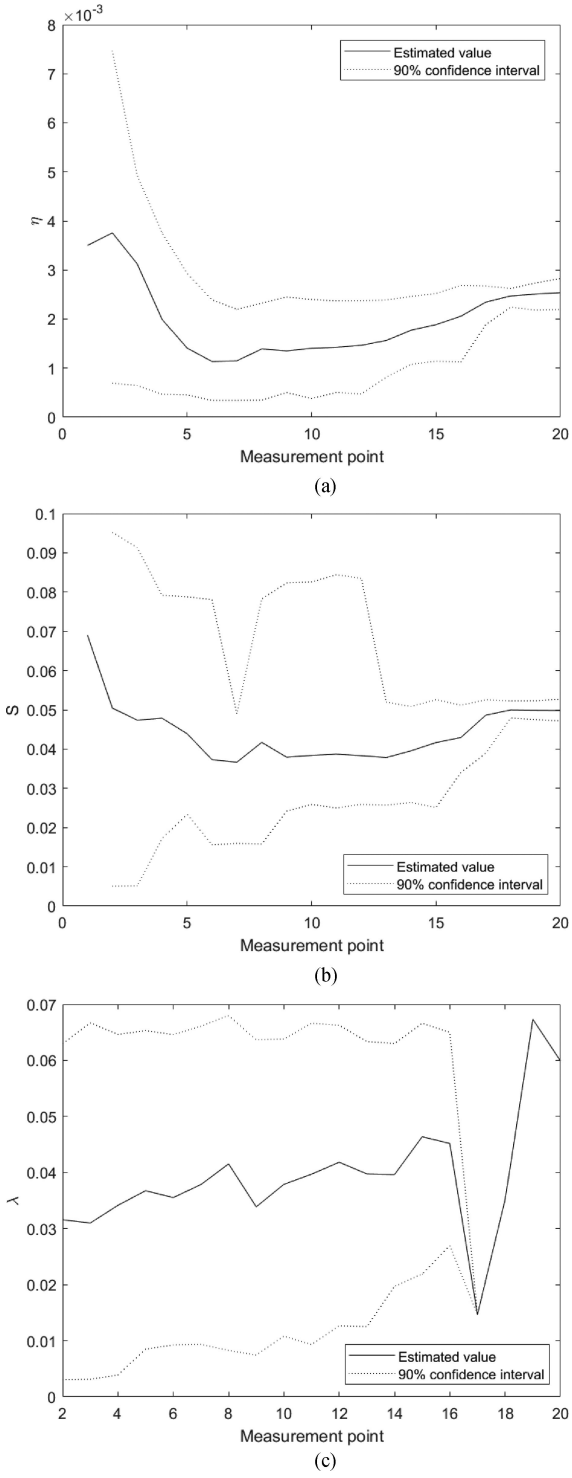

Fig. 14. Estimates of (a) the degradation rate, (b) the shock damage and (c) the shock intensity.

The results of the estimated model parameters are presented in Fig. 14. The estimated system degradation state and RUL are shown in Fig. 15. Due to the limited amount of degradation measurement data, the estimates of the model parameters are not as robust as the results of the numerical examples, but are still able to support a good fitting of the degradation path.

It is also worth noting that the estimate of system RUL has an increasing trend at the beginning of observation, as shown

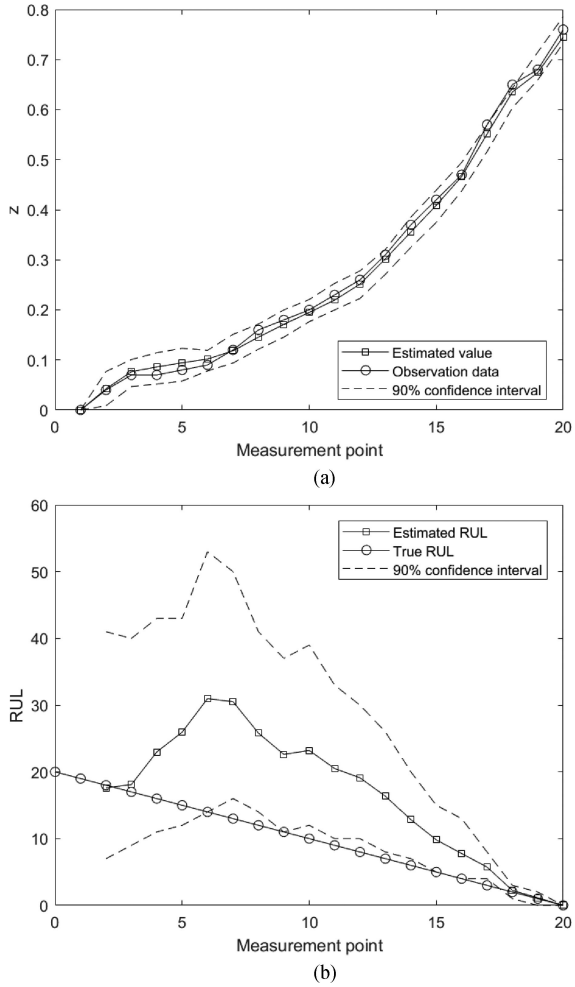

Fig. 15. Estimates of (a) the degradation level and (b) system RUL.

in Fig. 15: this is mainly because the degradation path shows an extremely low slope between the second and the sixth measurement points, which implies an optimistically estimated RUL compared to the true value. Also, due to the abnormal degradation trend between the second to the sixth measurement points, the corresponding 90% confidence intervals of RUL are relatively wide, which indicates a large variance in the samples.

VI. Conclusion

In this paper, a sequential Bayesian approach is developed for model parameters estimation and RUL prediction in presence of DCFP. In the developed model, the system degradation state and degradation model parameters are estimated by a PF algorithm and the shock process intensity is estimated by a MCMC algorithm using the MH sampler. With the MCMC algorithm, the posterior density of the system degradation state and model parameters are obtained using three types of data and knowledge: degradation observation data, prior knowledge of shock intensity, and system operation time. Considering the influence of both soft failures and hard failures, the system RUL is predicted by the minimum of system remaining TTSF and TTHF, in terms of probability density function. A comparison to an existing model in literature shows that the developed model provides

an efficient approach to estimate system state and RUL when shocks are unobservable, and generates more accurate results when systems are subject to hard failure.

In practice, estimation errors exist due to both measurement noises and the possible discrepancy between the state-space model used and the true physical failure process. To improve the accuracy of the prediction, developing more robust algorithms under the influence of the measurement noises is valuable work to be conducted in the future. In this paper, we only consider the dependency in the form that random shocks bring additional damage to the degradation process. In the future, the developed method can be extended to consider DCFPs with other types of dependencies. Moreover, dynamic reliability analysis considering large-scale failure dependencies such as propagative effects of failures [39] can be investigated.

REFERENCES

[1] Z. Zeng, R. Kang, and Y. Chen, "Using PoF models to predict system reliability considering failure collaboration," *Chin. J. Aeronaut.*, vol. 29, pp. 1294–1301, 2016.

[2] W. Li and H. Pham, "Reliability modeling of multi-state degraded systems with multi-competing failures and random shocks," *IEEE Trans. Rel.*, vol. 54, no. 5, pp. 297–303, Jun. 2005.

[3] X. Zhao, X. Guo, and X. Wang, "Reliability and maintenance policies for a two-stage shock model with self-healing mechanism". *Rel. Eng. Syst. Saf.*, vol. 172, pp. 185–194, 2018.

[4] H. Peng, Q. M. Feng, and D. W. Coit, "Reliability and maintenance modeling for systems subject to multiple dependent competing failure processes," *IIE Trans.*, vol. 43, pp. 12–22, 2011.

[5] Y. P. Wang and H. Pham, "A multi-objective optimization of imperfect preventive maintenance policy for dependent competing risk systems with hidden failure," *IEEE Trans. Rel.*, vol. 60, no. 4, pp. 770–781, Dec. 2011.

[6] Z. Wang, H. Z. Huang, Y. Li, and N. C. Xiao, "An approach to reliability assessment under degradation and shock process," *IEEE Trans. Rel.*, vol. 60, no. 4, pp. 852–863, Dec. 2011.

[7] L. Jiang, Q. M. Feng, and D. W. Coit, "Reliability and maintenance modeling for dependent competing failure processes with shifting failure thresholds," *IEEE Trans. Rel.*, vol. 61, no. 4, pp. 932–948, Dec. 2012.

[8] K. Rafiee, Q. M. Feng, and D. W. Coit, "Reliability modeling for dependent competing failure processes with changing degradation rate," *IIE Trans.*, vol. 46, pp. 483–496, 2014.

[9] K. Rafiee, Q. M. Feng, and D. W. Coit, "Reliability assessment of competing risks with generalized mixed shock models," *Rel. Eng. Syst. Saf.*, vol. 159, pp. 1–11, 2017.

[10] Y. H. Lin, Y. F. Li, and E. Zio, "Integrating random shocks into multi-state physics models of degradation processes for component reliability assessment," *IEEE Trans. Rel.*, vol. 64, no. 1, pp. 154–166, Mar. 2015.

[11] S. L. Song, D. W. Coit, and Q. M. Feng, "Reliability for systems of degrading components with distinct component shock sets," *Rel. Eng. Syst. Saf.*, vol. 132, pp. 115–124, 2014.

[12] L. Jiang, Q. M. Feng, and D. W. Coit, "Modeling zoned shock effects on stochastic degradation in dependent failure processes," *IIE Trans.*, vol. 47, pp. 460–470, 2015.

[13] V. Bagdonavicius, A. Bikelis, and V. Kazakevicius, "Statistical analysis of linear degradation and failure time data with multiple failure modes," *Lifetime Data Anal.*, vol. 10, pp. 65–81, 2004.

[14] J. Fan, S. G. Ghurye, and R. A. Levine, "Multicomponent lifetime distributions in the presence of ageing," *J. Appl. Probab.*, vol. 37, pp. 521–533, 2000.

[15] Z. S. Ye, L. C. Tang, and H. Y. Xu, "A distribution-based systems reliability model under extreme shocks and natural degradation," *IEEE Trans. Rel.*, vol. 60, no. 1, pp. 246–256, Mar. 2011.

[16] K. T. Huynh, I. T. Castro, A. Barros, and C. Bérenguer, "Modeling age-based maintenance strategies with minimal repairs for systems subject to competing failure modes due to degradation and shocks," *Eur. J. Oper. Res.*, vol. 218, pp. 140–151, 2012.

[17] K. T. Huynh, A. Barros, C. Bérenguer, and I. T. Castro, "A periodic inspection and replacement policy for systems subject to competing failure modes due to degradation and traumatic events," *Rel. Eng. Syst. Saf.*, vol. 96, pp. 497–508, 2011.

[18] N. C. Caballé, I. T. Castro, C. J. Pérez, and J. M. Lanza-Gutiérrez, "A condition-based maintenance of a dependent degradation-threshold-shock model in a system with multiple degradation processes," *Rel. Eng. Syst. Saf.*, vol. 134, pp. 98–109, 2015.

[19] M. Fan, Z. Zeng, E. Zio, and R. Kang, "Modeling dependent competing failure processes with degradation-shock dependence," *Rel. Eng. Syst. Saf.*, vol. 165, pp. 422–430, 2017.

[20] M. Fan, Z. Zeng, E. Zio, R. Kang, and Y. Chen, "A stochastic hybrid systems based framework for modeling dependent failure processes," *PloS One*, vol. 12, 2017, Art. no. e0172680.

[21] Z. Zeng, Y. Chen, E. Zio, and R. Kang, "A compositional method to model dependent failure behavior based on PoF models," *Chin. J. Aeronaut.*, vol. 30, pp. 1729–1739, 2017.

[22] S. Cheng, M. H. Azarian, and M. G. Pecht, "Sensor systems for prognostics and health management," *Sensors*, vol. 10, pp. 5774–5797, 2010.

[23] X. S. Si, W. Wang, C. H. Hu, and D. H. Zhou, "Remaining useful life estimation–a review on the statistical data driven approaches," *Eur. J. Oper. Res.*, vol. 213, pp. 1–14, 2011.

[24] J. Liu and E. Zio, "System dynamic reliability assessment and failure prognostics," *Rel. Eng. Syst. Saf.*, vol. 160, pp. 21–36, 2017.

[25] Zhai, Q. and Ye, Z. S., "RUL prediction of deteriorating products using an adaptive Wiener process model," *IEEE Trans. Ind. Informat.*, vol. 13, no. 6, pp. 2911–2921, Dec. 2017.

[26] H. K. Wang, Y. F. Li, Y. Liu, Y. J. Yang, and H. Z. Huang, "Remaining useful life estimation under degradation and shock damage," *Proc. Inst. Mech. Eng. O: J. Risk Rel.*, vol. 229, pp. 200–208, 2015.

[27] X. Ke, Z. Xu, W. Wang, and Y. Sun, "Remaining useful life prediction for non-stationary degradation processes with shocks," *Proc. Inst. Mech. Eng., O: J. Risk Rel.*, vol. 231, pp. 469–480, 2017.

[28] J. X. Zhang, C. H. Hu, X. He, X. S. Si, Y. Liu, and D. H. Zhou, "Lifetime prognostics for furnace wall degradation with time-varying random jumps," *Rel. Eng. Syst. Saf.*, vol. 167, pp. 338–350, 2017.

[29] G. Grimmett and D. Stirzaker, *Probability and Random Processes*. London, U.K.: Oxford Univ. Press, 2001.

[30] M. S. Hamada, A. Wilson, C. S. Reese, and H. Martz, *Bayesian Reliability*. Berlin, Germany: Springer Science & Business Media, 2008.

[31] M. S. Arulampalam, S. Maskell, N. Gordon, and T. Clapp, "A tutorial on particle filters for online nonlinear/non-Gaussian Bayesian tracking," *IEEE Trans. Signal Process.*, vol. 50, no. 2, pp. 174–188, Feb. 2002.

[32] J. Liu and M. West, *Combined Parameter and State Estimation in Simulation-Based Filtering, in Sequential Monte Carlo Methods in Practice*. New York, NY, USA: Springer, 2001, pp. 197–223.

[33] A. Tulsyan, B. Huang, R. B. Gopaluni, and J. F. Forbes, "On simultaneous on-line state and parameter estimation in non-linear state-space models," *J. Process Control*, vol. 23, pp. 516–526, 2013.

[34] Y. Hu, P. Baraldi, F. Di Maio, and E. Zio, "A prognostic approach based on particle filtering and optimized tuning kernel smoothing," in *Proc. 2nd Eur. Conf. Prognostics Health Manage. Soc.*, 2014.

[35] Z. Chen, "Bayesian filtering: From Kalman filters to particle filters, and beyond," *Statistics*, vol. 182, pp. 1–69, 2003.

[36] G. L. Jones and J. P. Hobert, "Honest exploration of intractable probability distributions via Markov chain Monte Carlo," *Statist. Sci.*, vol. 16, pp. 312–334, 2001.

[37] K. Baclawski. *Introduction to Probability with R*. Boca Raton, FL, USA: CRC Press, 2008.

[38] A. Agogino and K. Goebel, "Milling data set," BEST lab, UC Berkeley. Moffett Field, CA: NASA Ames Prognostics Data Repository, 2007. [Online]. Available: http://ti.arc.nasa.gov/project/prognostic-data-repository.

[39] P. Zhu, Y. Guo, S. Si, and J. Han, "A stochastic analysis of competing failures with propagation effects in functional dependency gates," *IISE Trans.*, vol. 49, no. 11, pp. 1050–1064, 2017.

Authors' photographs and biographies not available at the time of publication.